

Nonequilibrium phase transition by directed Potts particles

B. Kahng and S. Park

Department of Physics and Center for Advanced Materials and Devices, Konkuk University, Seoul 143-701, Korea

We introduce an interface model with q -fold symmetry to study the nonequilibrium phase transition (NPT) from an active to an inactive state at the bottom layer. In the model, q different species of particles are deposited or are evaporated according to a dynamic rule, which includes the interaction between neighboring particles within the same layer. The NPT is classified according to the number of species q . For $q = 1$ and 2, the NPT is characterized by directed percolation, and the directed Ising class, respectively. For $q \geq 3$, the NPT occurs at finite critical probability p_c , and appears to be independent of q ; the $q = \infty$ case is related to the Edwards-Wilkinson interface dynamics.

PACS numbers:05.70Fh,05.70Jk,05.70Ln

Recently, the problems of phase transitions in nonequilibrium systems have attracted considerable interest in the physical literature [1]. For example, the nonequilibrium phase transition (NPT) from an active state to an inactive state becomes one of the central issues in the field of nonequilibrium dynamics [2]. It was shown that the number of equivalent inactive (or absorbing) states characterizes universality classes for the NPT [3]. For example, NPT, occurring in the monomer-dimer model for the catalytic oxidation of CO [4], the contact process [5], *etc.*, has one absorbing state, and belongs to the directed percolation (DP) universality class [6]. Most of dynamic problems exhibiting the NPT with absorbing state, belong to this universality class. Meanwhile, there are a few exceptions: when there exist two absorbing states in the dynamic process, the critical behavior near the threshold of NPT is distinctive from that of the DP class, and belongs to the directed Ising (DI) class [3], equivalent to the class of parity-conserving branching-annihilating random walks [7]. The stochastic models in the DI class include, for example, the probabilistic cellular automata model [8], the interacting monomer-dimer model [9], the modified Domany-Kinzel model [10]. On the other hand, the scenario that the NPT can be classified according to the number of absorbing states is not complete since the NPT with more than two absorbing states is not known yet. In other words, the NPT in the directed q -state Potts (DPotts) class for $q \geq 3$ is not discovered yet. One reason may be from that for $q \geq 3$, active sites (kinks) generated at the boundary between different states domains appear more often than in the DI case. Thus, the absorbing state could not be reached for finite control parameter. Accordingly, it would be interesting to search for the NPT belonging to the DPotts class for $q \geq 3$.

Recently, the NPT has been considered in association with the roughening transition (RT) from a smooth to a rough phase. The NPT behavior appears at a particular reference height of the interface. For example, for the monomer deposition-evaporation (m-DE) model introduced by Alon *et al* [11], where evaporation of particle is not allowed on terrace, the reference height is the spontaneously selected bottom layer. The site where the

interface touches the reference height, called vacant site, corresponds to the active site of the NPT. In the active phase of the NPT, the interface fluctuates close to the reference height, being in a binded state, in which the interface is smooth. On the other hand, in the inactive phase, the interface is detached from the reference height, being in a unbinded state, and the interface is rough. Accordingly, RT accompanied by the binding-unbinding transition of the interface is related to the NPT at the reference height, which is characterized according to the number of symmetric states in the dynamic rule [12]. For the interface models with two-fold symmetry in their dynamic rule, which are the extensions of the m-DE model by assigning a couple of species to particles for one model [12], called the two-species model, and by enlarging the size of particles for the other model [13], called the dimer DE (d-DE) model, the dynamics at the reference height near the threshold of RT behaves similarly to the DI dynamics.

Both models contain the suppression effect against generating active sites, and the critical threshold of RT is considerably lower compared with the monolayer version. For the two-species model, the critical threshold is $p_c \approx 0.4480$ for the interface version, but $p_c \approx 0.7485$ for the monolayer version. In this Letter, we introduce an interface model with arbitrary q -fold symmetry, called the q -species model, and examine the NPT at the reference height for the cases $q = 3, 4, 5$ and ∞ . The result is compared with the previous one for $q = 1$ and 2. In addition, we study RT for each q . Interestingly, it is found that the NPT at the reference height *occurs* at finite deposition-probability for all cases, and their characteristics for $q \geq 3$ are different from the cases $q = 1$ and 2, but appear to be independent of q as long as $q \geq 3$. In particular, the interface model for the case $q = \infty$ is reduced to the restricted solid-on-solid (RSOS) model with deposition and evaporation processes. In this case, since RT occurs when the probabilities of deposition and evaporation are equal, the interface dynamics belongs to the Edwards-Wilkinson (EW) interface dynamics [14]. Accordingly, it is found that the NPT of the q -species model for $q \geq 3$ in one dimension is related to the EW class.

In the q -species model, q different species particles are deposited or evaporated on one dimensional substrate with periodic boundary condition. A site is first selected at random at which either deposition or evaporation of a particle is attempted with probability p and $1 - p$, respectively. In the attempt of deposition, one species is selected among the q species with equal weight $1/q$. Deposition or evaporation are realized under two conditions described below. First, the RSOS condition is imposed such that the height difference between nearest neighboring columns does not exceed one. Thus the attempt is realized as long as the RSOS condition is satisfied even after deposition or evaporation event. Secondly, the interaction between neighboring particles within the same layer is considered: When a particle of a certain species (e.g. A-species) is deposited on a hollow between particles, the deposition is not allowed when both of the neighboring particle on each side are of a common species (B-species), different from the dropping one (A-species). Meanwhile, a particle of a certain species (e.g. A-species) is not allowed for evaporation when it is sandwiched between particles of the same species (A-species) within the same layer. However, a particle can deposit or evaporate when two neighboring particles on each sides are of different species from one another, or one (or both) of the neighboring sites is (are) vacant. As $q \rightarrow \infty$, the probability of forming three particles in a row with the same species is zero. Thus, the secondary restriction is meaningless. Hence, the model is reduced to a random deposition-evaporation model under the RSOS condition. On the other hand, the initial substrate is flat where its height is referred as $h = 0$. The dynamics proceeds only for $h \geq 0$, so that evaporation of particles at $h = 0$ is not allowed.

Monte Carlo simulations are performed by varying the deposition probability p and system size L for the cases $q = 3, 4, 5$ and ∞ . We first discuss the dynamics occurring at the reference height, $h = 0$. We consider the density of the vacant site $\rho(p, t)$ at the reference height with varying time t at a certain deposition probability p . When p is small, particles form small-sized islands which disappear after their short lifetime and the growth velocity of interface is zero. The density $\rho(p, t)$ saturates at finite value as $t \rightarrow \infty$, as shown in Fig.1. As p increases, deposition increases and islands grow, until, above a critical value p_c , islands merge and fill new layers completely, giving the interface a finite growth velocity. Accordingly, RT occurs at p_c , and the NPT at the reference height occurs as well. The critical probability p_c , estimated for each q , is listed in Table 1. In particular, for $q = \infty$, the critical probability p_c is determined as $p_c = 0.5$, when the probabilities of deposition and evaporation are equal. For $p < p_c$, the saturated value $\tilde{\rho}(p)$ behaves as

$$\tilde{\rho}(p) \sim (p_c - p)^\beta, \quad (1)$$

with the order parameter exponent β . We estimated the exponent β from the data obtained from system size

$L = 500$, which is listed in Table 1. The numerical values for $q \geq 3$ do not seem to be close to each other, which makes it hard to conclude that the cases of $q \geq 3$ belong to the same universality class. However, the exponent β is hard to be measured precisely, because it is extremely sensitive to the estimated value p_c . Accordingly, the numerical value of β even for $q = 2$ is rather broadly ranged as can be noticed in Ref. [10]. On the other hand, for $p > p_c$, the density decreases to zero exponentially in the long time limit and at the critical threshold p_c , it decays algebraically as

$$\rho(p_c, t) \sim t^{-\beta/\nu_{\parallel}}. \quad (2)$$

The power, β/ν_{\parallel} , is measured in Fig.1 and is tabulated in Table 1. The values are reasonably close to one another for $q \geq 3$, but considerably larger than the values for $q = 1$ and 2. This result suggests that the number of species is unimportant for $q \geq q_c \equiv 3$. On the other hand, we need to discuss the relation between the vacant sites and the kinks which are the domain boundaries between different species, because the kinks are indeed active sites in the directed Potts dynamics. We measure the kink density $\rho_K(p_c, t)$ by counting the sites with height equal to one and whose neighbors are different species, which behaves similarly to $\rho(p_c, t)$, as shown in Fig.2. Thus we confirm that the vacant site density is equivalent to the active site density in the q -species model. Finally, we simulate the monolayer version of the q -species model, and find that the system does not exhibit NPT and is always in the active state for finite p . A similar behavior was found in the three-species monomer-monomer reaction model introduced by Bassler and Browne [15], in which the system is always in a reactive phase when the absorption rates for each species are identical.

The density $\rho(p, t)$ can be thought as the return probability $P_0(p, t)$ of interface height $h(x, t)$ to its initial height $h(x, t) = 0$ after passing time t , averaged over the substrate position x . The subscript 0 means that the time is measured from $t = 0$. In general, $P_0(p, t)$ is different from the first return probability $F_0(p, t)$ of the interface height to its initial height, which decays as $F_0(p, t) \sim t^{-\theta}$ where θ is called the persistent exponent [16]. For the EW interface under the given boundary condition at $h = 0$, we obtain that $F_0(p_c, t) \sim t^{-0.75}$, similar to $P_0(p_c, t)$. Hence, the power β/ν_{\parallel} for $q = \infty$ is related to the persistent exponent for the EW interface.

Next, let us consider the size dependence of $\rho(p_c, t)$. To do so, we study the averaged density $\rho^{(s)}(p_c, t)$ over the active runs which contain at least one vacant site at the reference height. Since $\rho(p_c, t)$ decays as Eq.(2) at p_c , the vacant sites disappear completely as $t \rightarrow \infty$. There exists a characteristic time τ such that every run is active up to the time τ , while for $t > \tau$, it is active with probability less than one and proportional to $\rho(p_c, t)$, leading to the saturation of $\rho^{(s)}(p_c, t)$, as shown in Fig.3. This fact implies that for $t > \tau$, when vacant sites exist, their number should be of order of unity. Once they are occupied, the sample falls into the inactive state, because other sites

are covered by particles on upper layer. Hence, the density follows $\rho(p_c, \tau) \approx 1/L$. The characteristic time τ depends on system size L as $\tau \sim L^z$ with the dynamic exponent $z = \nu_{\parallel}/\nu_{\perp}$. According to the scaling theory, the saturated value, $\tilde{\rho}^{(s)}(p_c)$ is written as

$$\tilde{\rho}^{(s)}(p_c) \sim L^{-\beta/\nu_{\perp}}. \quad (3)$$

The power β/ν_{\perp} is found to be ≈ 1 , as predicted. Therefore, the dynamic exponent z is obtained to be between 1.32 and 1.41, which deviates from the value $z_{EW} = 2$ for the interface dynamics. The origin of this discrepancy may be that the dynamics at the reference level is affected by the boundary at $h = 0$.

Let us consider the dynamics of interface above the reference height. We examine the interface fluctuation width, $W^2(L, t) = \frac{1}{L} \sum_x h^2(x, t) - \left(\frac{1}{L} \sum_x h(x, t)\right)^2$ at p_c . Contrary to the cases $q = 1$ and 2 , W^2 exhibits the power-law behavior as shown in Fig.4,

$$W^2(L, t) \sim \begin{cases} t^{2\zeta}, & \text{for } t \ll L^{\chi/\zeta}, \\ L^{2\chi}, & \text{for } t \gg L^{\chi/\zeta}, \end{cases} \quad (4)$$

where ζ and χ are the growth and the roughness exponents, respectively. The exponents ζ and χ for $q \geq 3$ are obtained numerically as $\zeta \approx 0.22, 0.23, 0.23$ and 0.24 , and $\chi \approx 0.46, 0.48, 0.46$ and 0.48 for $q = 3, 4, 5$ and ∞ , respectively. These values are close to the EW values, $\zeta = 1/4$ and $\chi = 1/2$. We also examine the height-height correlation function, $C^2(r) = \langle (h(r) - h(0))^2 \rangle \sim r^{2\chi'}$ in the long time limit. The exponent χ' is consistent with χ . For $p > p_c$, the scaling of the interface width belongs to the Kardar-Parisi-Zhang universality class [17].

We also generalize the d-DE model into the trimer case, called the t-DE model, where a trimer is deposited with probability p or evaporated with probability $1 - p$ according to a rule similar to the d-DE model. Note that the t-DE model is different from the model introduced by Stinchcombe *et.al.* [18] in the two aspects: the former (latter) model is an interface (monolayer) model, and evaporation on terrace is prohibited (allowed). As shown in Fig.5, there exists a critical deposition probability p_c such that for $p < p_c$, the density of the vacant sites at the bottom layer is saturated, whereas for $p \geq p_c$, it decays algebraically. Note that the behavior of the exponential-type decay for $p > p_c$ does not appear in the t-DE model. The exponent, β/ν_{\parallel} is obtained to be ≈ 0.38 , which is almost half of the value for the 3-species model, which is also the case for $q = 2$. On the other hand, the dynamic exponent $z \approx 2.47$ is obtained by measuring the characteristic time for finite-size cutoff. This value is inconsistent with the one for the q -species model. Accordingly, further study for the dynamic exponent z is required. Detailed numerical results for the t-DE model and its generalization into arbitrary q -mer case will be published elsewhere [19].

In summary, we have introduced the q -species model, which is an interface model exhibiting RT accompanied

by the binding-unbinding transition with respect to the reference height. The NPT occurring at the reference height has been examined numerically for $q = 3, 4, 5$ and ∞ . We found that the NPT occurs at finite p_c for all the cases of q , which is remarkable, because the NPT for $q \geq 3$ has never been found before. For $q \geq q_c = 3$, the number of species is unimportant, and the NPT independent of q is related to the EW interface dynamics via the return probability of interface to its initial height. We measured the critical exponents for NPT and RT. We also considered the t-DE model with three-state symmetry, and compared the result with the three-state model.

The authors wish to thank H. Park and J.D. Noh for helpful discussions. This work was supported in part by the Korea Research Foundation (98-001-D00280 & 98-015-D00090).

-
- [1] For a review, see, V. Privman, *Nonequilibrium Statistical Mechanics in One Dimension* (Cambridge University Press, Cambridge, 1996).
 - [2] J. Marro and R. Dickman, *Nonequilibrium Phase Transitions* (Cambridge University Press, Cambridge, 1997).
 - [3] H. Park and H. Park, *Physica A* **221**, 97 (1995).
 - [4] R.M. Ziff, E. Gulari and Y. Barshad, *Phys. Rev. Lett.* **56**, 2553 (1985).
 - [5] T.E. Harris, *Ann. Prob.* **2**, 969 (1974); T.M. Liggett, *Interacting Particle Systems* (Springer-Verlag, New York, 1985)
 - [6] G. Deutscher, R. Zallen and J. Adler, *Percolation Structures and Processes* *Ann. Isr. Phys. Soc.* **5** (Adam Hilger, Bristol, 1983).
 - [7] H. Takayashu and A. Y. Tretyakov, *Phys. Rev. Lett.* **68**, 3060 (1992).
 - [8] P. Grassberger, F. Krause and T. von der Twer, *J. Phys. A* **17**, L105 (1984).
 - [9] M.H. Kim and H. Park, *Phys. Rev. Lett.* **73**, 2579 (1994).
 - [10] H. Hinrichsen, *Phys. Rev. E* **55**, 219 (1997).
 - [11] U. Alon, M.R. Evans, H. Hinrichsen and D. Mukamel, *Phys. Rev. Lett.* **76**, 2746 (1996); *Phys. Rev. E* **57**, 4997 (1998).
 - [12] S. Park and B. Kahng (cond-mat/9807193).
 - [13] H. Hinrichsen and G. Ódor, *Phys. Rev. Lett.* **82**, 1205 (1999).
 - [14] S.F. Edwards and D.R. Wilkinson, *Proc. R. Soc. Lond. A* **381**, 17 (1982).
 - [15] K.E. Bassler and D.A. Browne, *Phys. Rev. Lett.* **77**, 4094 (1996); *Phys. Rev. E* **55**, 5225 (1997).
 - [16] J. Krug, H. Kallabis, S.N. Majumdar, S.J. Cornell, A.J. Bray, and C. Sire, *Phys. Rev. E* **56**, 2702 (1997).
 - [17] M. Kardar, G. Parisi and Y.C. Zhang, *Phys. Rev. Lett.* **56**, 889 (1986).
 - [18] R.B. Stinchcombe and M.D. Grynberg, and M. Barma, *Phys. Rev. E* **47**, 4018 (1993).
 - [19] B. Kahng and S. Park (unpublished).

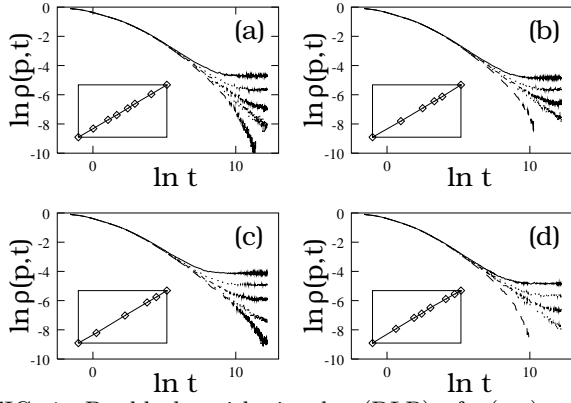


FIG. 1. Double logarithmic plot (DLP) of $\rho(p, t)$ versus time t (a) for $q = 3$ at $p = 0.4904, 0.4910, 0.4913, 0.4914(= p_c)$ and 0.4917 from the top. (b) for $q = 4$ at $p = 0.5020, 0.5024, 0.5026, 0.5027(= p_c)$, and 0.5031 from the top. (c) for $q = 5$ at $p = 0.5051, 0.5059, 0.5063, 0.5065(= p_c)$, and 0.5066 from the top. (d) for $q = \infty$ at $p = 0.4993, 0.4997, 0.4999, 0.5000(= p_c)$, and 0.5005 from the top. All data are obtained for $L = 500$, averaged over 1000 realizations. Insets: DLP of $\tilde{\rho}(p)$ versus ϵ for each q . The solid line is a guideline to the eye.

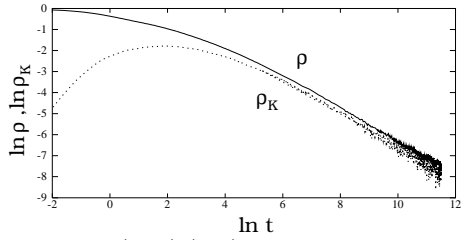


FIG. 2. DLP of $\rho(p_c, t)$ (top) and the kink density $\rho_K(p_c, t)$ versus time t at p_c . The numerical results are obtained for $L = 1000$, averaged over 1000 realizations.

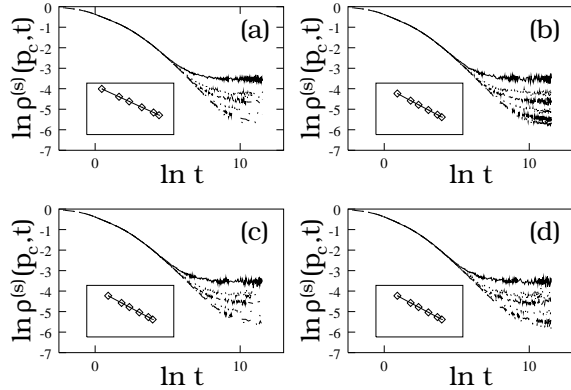


FIG. 3. DLP of $\rho^{(s)}(p_c, t)$ versus time t at p_c for different system sizes $L = 100, 200, 300, 500, 800$ and 1000 from the top for (a) $q = 3$, (b) $q = 4$, (c) $q = 5$, and (d) $q = \infty$. The data are averaged over 1000 realizations. Insets: DLP of $\tilde{\rho}^{(s)}(p_c)$ versus L for each q . The solid line is a guideline to the eye.

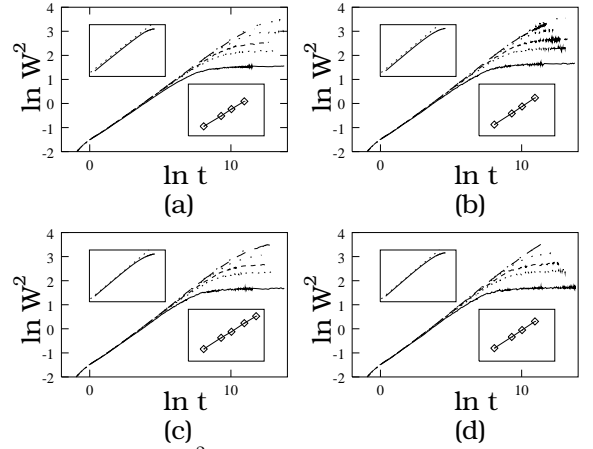


FIG. 4. DLP of W^2 versus time t at p_c for different system sizes $L = 100, 200, 300, 500, 800$ and 1000 from the bottom for (a) $q = 3$, (b) $q = 4$, (c) $q = 5$, and (d) $q = \infty$. Insets-left: DLP of $C^2(r)$ versus distance r for $L = 500$ for each q . The dashed line is a guideline to the eye. Insets-right: DLP of the saturated value of W^2 versus L for each q . The solid line is a guideline to the eye. All the data are averaged over 1000 realizations

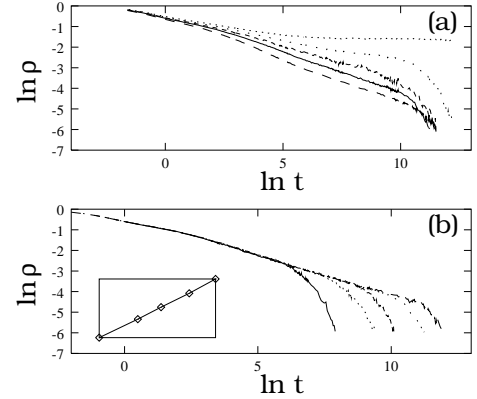


FIG. 5. (a) DLP of $\rho(p, t)$ versus time t for the t -DE model at $p = 0.32, 0.34, 0.36, 0.38(= p_c)$, and 0.42 from the top. The data are obtained from system size $L = 500$, averaged over 500 realizations. (b) DLP of $\rho(p_c, t)$ versus time t for various system sizes $L = 99, 198, 300, 498$ and 798 from the left. The data are averaged over 500 realizations. Inset: DLP of the characteristic time τ versus system size L . The solid line is a guideline to the eye.

TABLE I. The estimated values of $p_c, \beta, \beta/\nu_{\parallel}, \beta/\nu_{\perp}$, and z for various q . The data for the cases of $q = 1$ and $q = 2$ are quoted from Refs.12 and 13, respectively.

q	p_c	β	β/ν_{\parallel}	β/ν_{\perp}	z
1	0.189	0.28	0.16	0.25	1.56
2	0.4480	0.88	0.59	0.97	1.64
3	0.4914	1.01(3)	0.75(1)	0.99(1)	1.32
4	0.5027	0.94(2)	0.73(1)	0.99(1)	1.36
5	0.5065	0.91(3)	0.70(1)	0.99(1)	1.41
∞	0.5000	0.95(3)	0.75(1)	0.99(1)	1.32